Evaluating multiple determinants of the structure of plant–animal mutualistic networks*

Diego P. Vázquez[1,2], Natacha P. Chacoff[1] and Luciano Cagnolo[3]

1. Instituto Argentino de Investigaciones de las Zonas Áridas, CONICET, CC 507, 5500 Mendoza, Argentina (dvazquez@mendoza-conicet.gov.ar, nchacoff@mendoza-conicet.gov.ar)

2. Instituto de Ciencias Básicas, Universidad Nacional de Cuyo, Centro Universitario, M5502JMA Mendoza, Argentina

3. IMBIV and Centro de Investigaciones Entomolgicas de Córdoba, CONICET–Universidad Nacional de Córdoba, FCEFN, Av. Vélez Sarsfield 1611, X5016GCA Córdoba, Argentina (lcagnolo@efn.uncor.edu)

Running title: The structure of mutualistic networks
Manuscript type: Report

Abstract

The structre of mutualistic networks is likely to result from the simultaneous influence of neutrality and the constraints imposed by complementarity in species phenotypes, phenologies, spatial distributions, phylogenetic relationships and sampling artifacts. We develop a conceptual and methodological framework to evaluate the relative contributions of these potential determinants. Applying this approach to the analysis of a plant–pollinator network, we show that information on relative abundance and phenology suffices to predict several aggregate network properties (connectance, nestedness, interaction evenness and interaction asymmetry). However, such information falls short of predicting the detailed network structure (the frequency of pairwise interactions), leaving a large amount of variation unexplained. Taken together, our results suggest that both relative species abundance and complementarity in spatio–temporal distribution contribute substantially to generate observed network patters, but that this information is by no means sufficient to predict the occurrence and frequency of pairwise interactions. Future studies could use our methodological framework to evaluate the generality of our findings in a representative sample of study systems with contrasting ecological conditions.

Keywords: forbidden links; neutrality; phenotipic complementarity; phylogenetic signal; pollination; Villavicencio network

---

*Article in press in *Ecology*

1

Introduction

There is growing interest in the study of networks of interacting plant and animal mutualists. This interest stems from the realization that considering the community context is important to understand the ecological and evolutionary implications of mutualistic interactions (Strauss and Irwin, 2004). Studies of mutualistic networks have uncovered some apparently general structural properties, such as the skewed distribution of links per species (many species with few links and few species with many links; Jordano et al., 2003; Vázquez and Aizen, 2003), the nested organization of the interaction matrix (Bascompte et al., 2003) and the frequent occurrence of asymmetric interactions (Vázquez and Aizen, 2004; Bascompte et al., 2006).

Recent discussion about the potential ecological and evolutionary determinants of these structural patterns has centered around the relative importance of neutrality vs. the so-called "forbidden links". The neutrality hypothesis posits that network patterns result from the fact that individuals interact randomly, so that abundant species interact more frequently and with more species than rare species (Dupont et al., 2003; Ollerton et al., 2003; Vázquez et al., 2007). The forbidden links hypothesis posits that network patterns result from constraints to interactions imposed by the complementarity in species phenotypes, phenologies, spatial distributions and phylogenetic relationships (Jordano et al., 2003; Rezende et al., 2007; Santamaría and Rodríguez-Gironés, 2007; Stang et al., 2007). For example, two species cannot interact if their phenologies do not overlap, regardless of what their abundance alone predicts.

Available evidence suggests that both neutrality and forbidden links contribute to some extent to determine network structure (Bascompte and Jordano, 2007; Vázquez et al., 2009). For example, Vázquez et al. (2007) have shown that relative species abundance partly (but not entirely) explains the observed asymmetry in the strength of pairwise interactions, whereas Stang et al. (2007) showed that information on both abundance and morphological traits of plants and pollinators are needed to predict asymmetry and nestedness in binary networks. Several recent studies have also shown that phenologies and inter-annual dynamics of plant and animal species influence network structure (Basilio et al., 2006; Alarcón et al., 2008; Olesen et al., 2008; Petanidou et al., 2008). In a similar vein, a recent simulation study has shown that the degree of mixing resulting from the spatial aggregation of plant individuals and the scale of animal movement decisions has strong influences on network structure (Morales and Vázquez, 2008). The key unanswered question is how important each of these processes is in determining network structure. Here we develop a conceptual and methodological framework to answer this question and apply it to investigate the determinants of a plant–pollinator network.

Consider a mutualistic network depicted as an interaction matrix $\mathbf{Y}$ with I rows and J columns corresponding to the plant and animal species in the network, respectively, and a positive integer in cell y_{ij} representing the number of interactions recorded between plant i and animal j. This matrix is a function of multiple interaction probability matrices of the same size as $\mathbf{Y}$, determined by relative species abundance ($\mathbf{N}$), temporal ($\mathbf{T}$) and spatial overlap ($\mathbf{S}$) and phenotypic traits of interacting species ($\mathbf{K}$). The effects of these factors on $\mathbf{Y}$ can be constrained by the phylogenetic relationships among plants ($\mathbf{P_p}$) and animals ($\mathbf{P_a}$) (Rezende et al., 2007). In addition, detection probabilities of interactions resulting from sampling effects ($\mathbf{E}$) can also influence the observed network (Blüthgen et al., 2008). Thus,

$$\mathbf{Y} = f(\mathbf{N}, \mathbf{T}, \mathbf{S}, \mathbf{K}, \mathbf{P_p}, \mathbf{P_a}, \mathbf{E}). \tag{1}$$

Below we use this conceptual framework to evaluate the contribution of abundance, spatial and temporal overlap and phylogenetic relatedness among species on the structure of a plant–pollinator network. Specifically, we address the following questions: (i) To what extent do relative abundance and spatio–temporal overlap predict aggregate network statistics (connectance, nestedness, interaction strength evenness and the distribution of interaction strength asymmetries)? (ii) To what extent do these factors predict pairwise interaction frequencies in the interaction matrix? (iii) Is there any detectable phylogenetic signal in the interaction matrix, suggesting that the influence of abundance and spatio–temporal overlap on network structure could have resulted from phylogenetic constraints imposed by the phylogenetic relationships among plants and among animals?

Materials and Methods

Study system Data come from a plant–pollinator network from the Monte desert at Villavicencio Nature Reserve (32° 32' S, 68° 57' W, 1270 masl), Mendoza, Argentina. We worked in four 1 ha plots, separated by 1-2 km. Predominant vegetation is a tall shrubland dominated by *Larrea divaricata*, *Zuccagnia punctata*, *Prosopis flexuosa*, *Condalia microphylla*, *Acantholippia seriphoides* and *Opuntia sulphurea* (Roig, 1972). We give only a summarized description of field methods here; further details can be found in the original publication describing the network (Chacoff et al., 2009).

Plant–pollinator interactions Flower visiting insects were observed on plant species in weekly surveys in two consecutive flowering seasons (2006 and 2007) between September and January (2006) or December (2007). We attempted to sample plant–pollinator interactions in the whole community as comprehensively as possible, recording interactions between 41 plant species and 97 insect species. With these data we constructed a quantitative plant–pollinator interaction matrix $\mathbf{Y} = [y_{ij}]$, with rows corresponding to plant species and columns to pollinator species; cell entries y_{ij} are integers representing the number of flowers of plant species i visited by pollinator species j (Fig. 1a). This is the network we want to predict.

Species abundance Plant abundance was assessed in weekly surveys along five fixed 50 m × 2 m transects in the four sites, where we recorded the number of individuals of each entomophilous species and, for a subset of individuals, the number of flowers per individual. We also collected three fresh flowers from ten individuals of each species to estimate the number of pollen grains produced per flower. We attempted to obtain nectar from flowers, but we failed for most plant species; flowers in this system usually have very small standing volumes of nectar. With these data we estimated the density of individuals, density of flowers (density of individuals × flowers per individual) and density of pollen (density of individuals × flowers per individual × pollen grains per flower) for each species at each site. Arguably, density of flowers is the most appropriate measure of abundance from the flower visitors' perspective: it is a better estimate of resource abundance than density of individual plants (because there is high variation among plant species in the mean number of flowers per individual) and focuses on the flower as the resource unit for both pollen and nectar. However, because different studies use different measures of abundance, we considered the three measures to evaluate how the choice of a particular measure affects our results.

124 Because flowers of most species usually last less than a week, and because we were
125 interested in an overall measure of abundance, we summed density across weeks and sites
126 to obtain an overall estimate of abundance of each species. Thus, a plant species could be
127 abundant because it produced many flowers in a short period or because it produced few
128 flowers over a long period. These two forms of abundance were then distinguished by
129 incorporating temporal and spatial structure in our network model, as described below
130 (see Spatial and temporal overlap).

131 Insect abundance was defined as the total number of visits made by a particular insect
132 species to any plant species (that is, the column sum of the interaction matrix), as done
133 in previous studies (see, e.g., Vázquez et al., 2007).

Spatial and temporal overlap To quantify spatial and temporal overlap of plant and
135 pollinator species, we first compiled matrices of temporal and spatial occurrences, with
136 species in rows and date or site in columns, and cells with ones for presences and zeros for
137 absences. We thus had one temporal and one spatial occurrence matrix for plants, $\mathbf{O}_p^t$
138 and $\mathbf{O}_p^s$, and one of each for animals, $\mathbf{O}_a^t$ and $\mathbf{O}_a^s$. We then used matrix multiplication to
139 calculate spatial and temporal overlap matrices between plants and animals, $\mathbf{S} = \mathbf{O}_p^s \mathbf{O}_a^{s\prime}$
140 and $\mathbf{T} = \mathbf{O}_p^t \mathbf{O}_a^{t\prime}$, where the prime symbol indicates the transpose of a matrix o vector.

Calculation of interaction probabilities We calculated interaction probability
142 matrices expected under the assumptions that interactions were determined solely by
143 relative species abundances, temporal overlap and spatial overlap. For relative abundance,
144 interaction probability between a plant species i and a pollinator species j is simply the
145 product of their relative abundances. In matrix notation, the interaction probability
146 matrix expected from relative abundances is $\mathbf{N} = \mathbf{n}_p \mathbf{n}_a{}'$. For temporal and spatial
147 overlap, we used overlap matrices $\mathbf{T}$ and $\mathbf{S}$ normalized so that their elements added up to
148 one, so as to transform them into probabilities. (For simplicity, we call these normalized
149 matrices $\mathbf{T}$ and $\mathbf{S}$ hereafter.) Thus, the greater the temporal or spatial overlap of two
150 species, the greater their probability of interaction; species with no temporal or spatial
151 overlap had zero probability of interaction. We also calculated combined probabilities as
152 the element-wise multiplication of matrices $\mathbf{N}$, $\mathbf{T}$ and $\mathbf{S}$, again normalizing the resulting
153 matrices so that their elements added up to one. These combined matrices represent the
154 expected probability under the joint influence of more than one of these factors. For
155 example, $\overline{\mathbf{NS}}$ denotes the combined abundance–spatial overlap probability matrix, and
156 represents the interaction probabilities expected if species interact proportionally to their
157 abundances given that they co-occur at a particular site. Thus, we had seven probability
158 matrices with all possible combinations of relative abundance and temporal and spatial
159 overlap: $\mathbf{N}$, $\mathbf{T}$, $\mathbf{S}$, $\overline{\mathbf{NT}}$, $\overline{\mathbf{NS}}$, $\overline{\mathbf{TS}}$ and $\overline{\mathbf{NTS}}$. In addition, we defined an eighth probability
160 matrix in which all pairwise interactions had the same probability $1/IJ$ of occurrence,
161 where I and J are the numbers of plant and animal species in the network; this
162 probability matrix, termed "Null" below (see Figs. 2 and 3), is taken as a benchmark null
163 model for comparison with the other seven probability matrices.

Analysis of aggregate network statistics We considered four aggregate network
165 statistics frequently used in the analysis of plant–animal mutualisitic networks:
166 connectance, nestedness, interaction evenness and interaction asymmetry. Connectance is
167 the proportion of realized interspecific links, defined as $C = L/(IJ)$, where L is the
168 number of non-zero entries in the binary interaction network and I and J are, as above,

the numbers of plant and animal species in the network. Nestedness is the tendency of specialized species to interact with a subset of the interaction partners of more generalized species or, more precisely, the degree of symmetry in the distribution of unexpected absences and presences on each side of the boundary line defining perfect nestedness (Almeida-Neto et al., 2007). Thus, a nestedness value of 1 represents complete lack of symmetry (perfect nestedness), while a value of 0 represents the highest symmetry in the distribution of unexpected presences and absences, with absolute randomness falling somewhere in between 0 and 1. Nestedness was calculated with the BINMATNEST algorithm proposed by Rodríguez-Gironés and Santamaría (2006), implemented in the bipartite package (Dormann et al., 2008) of R statistical software (R Development Core Team, 2007); the BINMATNEST algorithm overcomes several limitations of the widely used nestedness temperature calculator developed by Atmar and Patterson (1993). Following Tylianakis et al. (2007), interaction evenness was defined as Shannon's index, $H = p_{ij} \log_2 p_{ij} / \log_2 F$, where F is the total number of plant–pollinator interactions in the matrix (see eq. 2 below) and p_{ij} is the proportion of those interactions involving plant i and pollinator j. An uneven network is one with high skewness in the distribution of interaction frequencies. Interaction asymmetry for a given species was defined as $A_i = \frac{\sum_j d_{ij}}{k_i}$, where k_i is the degree of species i (i.e., the number of species with which i interacts) and d_{ij} is a measure of the symmetry of the strength of the pairwise interaction between i and j (Vázquez et al., 2007); as in previous publications, we used interaction frequency as a surrogate of interaction strength (see Vázquez et al., 2005; Bascompte et al., 2006; Vázquez et al., 2007).

We used a randomization algorithm implemented in R (see Supplement) to evaluate to what extent interaction probabilities derived from relative abundance and spatial and temporal overlap of species occurrences predicted the observed aggregate network statistics. The algorithm assigned the total number of interactions originally observed in the interaction matrix according to the seven probability matrices defined by all possible combinations of abundance and temporal and spatial overlap (see Interaction probabilities above), with the only constraint that each species received at least one interaction.

Likelihood analysis of pairwise interaction probabilities   We used a likelihood approach to evaluate the ability of abundance, temporal overlap and spatial overlap to predict the detailed structure of the interaction matrix. Consider the observed interaction matrix $\mathbf{Y}$ and a probability matrix $\mathbf{X}$, whose entries x_{ij} are the probabilities of occurrence for each pairwise interaction; we want to evaluate whether those probabilities match the observed frequencies of interaction. This evaluation can be done by calculating the likelihood of probability matrix $\mathbf{X}$ given the data ($\mathbf{Y}$). We assumed that the pairwise probability of interaction between a plant i and a pollinator j followed a multinomial distribution. Thus, the likelihood of probability matrix l given the data is

$$\mathscr{L}_l = \frac{F!}{\prod_{i=1}^{I} \prod_{j=1}^{J} y_{i,j}!} \prod_{i=1}^{I} \prod_{j=1}^{J} x_{ijl}^{y_{ij}} \tag{2}$$

where F is the total number of observed interactions (i.e., the sum of the elements of matrix $\mathbf{Y}$), and I and J are the total number of animals and plants in $\mathbf{Y}$, respectively. We calculated this likelihood using function dmultinom in the stats package of R. We then calculated Akaike's Information Criterion as $\mathrm{AIC}_l = \mathbf{L}_l - 2k_l$, where k_l is the number of parameters involved in generating probability matrix l. The number of

212 parameters was defined as the number of factors contributing to generate a particular
213 probability matrix; thus, matrix $\mathbf{N}$ has one parameter, $\overline{\mathbf{TS}}$ has two and $\overline{\mathbf{NTS}}$ has three.

214 **Phylogenetic analysis**   Ideally, we would like to incorporate phylogenetic effects into
215 our conceptual framework, constructing a phylogenetic probability matrix as we did with
216 abundance, temporal overlap and spatial overlap. Regrettably, incorporation of
217 phylogenetic effects was not possible because we found no way of predicting pairwise
218 interactions from the plant and pollinator phylogenies alone, without reference to the
219 observed interaction matrix. Alternatively, we evaluated the strength of the phylogenetic
220 signal of the two phylogenies on the interaction matrix with the method developed by
221 Ives and Godfray (2006): a linear model approach to fit the phylogenetic
222 variance–covariance matrix to the interaction matrix. Using this method we calculated
223 the independent signals of the plant (d_p) and animal (d_a) phylogenies and the strength of
224 the signal of both phylogenies combined $(\mathrm{MSE_d})$ (Appendix A).

225 Results

226 **Aggregate network statistics**   No probability matrix predicted connectance and
227 interaction evenness values whose confidence intervals included observed values of these
228 statistics (Fig. 2a, c). However, predictions from probability matrices $\overline{\mathbf{NTS}}$ and $\overline{\mathbf{NT}}$, $\overline{\mathbf{NS}}$
229 and $\mathbf{N}$ were extremely close to observed connectance and interaction evenness. Observed
230 nestedness was included within the randomization confidence intervals of the same four
231 probability matrices (Fig. 2b). A similar result was observed for interaction asymmetry
232 for pollinators (Fig. 2d), but not for plants (Fig. 2e). In the latter case, observed average
233 asymmetry was close to zero (predominantly symmetric interactions) and similar to that
234 predicted by the null model that assumes that all species have the same probability of
235 interaction. Highly negative asymmetry in pollinators and high symmetry for plants
236 matches previous results for other interaction networks (Vázquez et al., 2007). Thus,
237 with the exception of asymmetry for plants, information on abundance and temporal
238 overlap suffices to simulate interaction networks whose aggregate structure resembles very
239 closely the structure of the observed matrix $\mathbf{Y}$. This result was the same regardless of the
240 measure of abundance used (i.e., density of individuals, individuals × flowers or
241 individuals × flowers × pollen; result not shown).

242 **Frequency of pairwise interactions**   Taking density of flowers as our measure of
243 plant abundance (which, as explained above, is arguably the most appropriate measure),
244 the combined probability matrix $\overline{\mathbf{NT}}$ had the lowest dAIC value, with a difference with
245 the next best-fitting probability matrix $\overline{\mathbf{TS}}$ of 156, and several orders of magnitude with
246 the null model (Fig. 3b). However, this best-fitting probability model was also orders of
247 magnitude worse than the perfect fit obtained by fitting the interaction matrix to itself.
248 These results suggest that abundance and temporal overlap are useful to predict part of
249 the detailed structure of the interaction matrix, but that we are far from an accurate
250 prediction, with much unexplained variation.
251   The latter conclusion can be visualized by comparing the observed interaction matrix
252 (Fig. 1a) with an example of a matrix resulting from the randomization procedure with
253 the $\overline{\mathbf{NT}}$ probability matrix (Fig. 1b). For example, although the two randomized
254 matrices look roughly similar to the observed matrix in terms of connectance and
255 nestedness, it is obvious that the most frequently observed interactions are not those

predicted to occur most frequently by $\overline{\mathbf{NT}}$. Thus, although knowledge of abundance and phenology allows us to predict aggregate network properties with high accuracy, we do rather poorly at predicting the detailed occurrence of pairwise interactions.

Unlike results for aggregate network statistics, using a different measure of abundance affects our ability to predict pairwise interactions (Figs. 3a, c): $\overline{\mathbf{NT}}$ is now in sixth place, doing particularly badly when abundance is measured as density of pollen, almost as badly as the null model. Notice that because matrices not including abundance are the same between Figs. 3a, b and c, results can be directly compared, indicating that the $\overline{\mathbf{NT}}$ probability matrix when abundance is measured as density of flowers provides the overall best fit.

Phylogenetic signal   The independent phylogenetic signal of the insect phylogeny was weak ($d_a = 0.067$) and its confidence interval overlapped zero (95% confidence limits: [0, 0.286]). The independent plant phylogenetic signal was stronger ($d_p = 0.327$) and did not overlap zero (95% confidence limits: [0.189, 0.532]). The overall strength of the phylogenetic signal for the linear model fitted to the actual data ($\mathrm{MSE_d} = 250.05$) was much closer to that found under the assumption of no phylogenetic covariances (the "star" phylogeny: $\mathrm{MSE_{star}} = 269.29$) than for the assumption of maximum phylogenetic signal (Brownian motion evolution: $\mathrm{MSE_b} = 420.61$). Taken together, these results suggest that only phylogenetic relationships among plants, not insects, impose some structure on the interaction matrix $\mathbf{Y}$, but that the overall phylogenetic signal is extremely weak.

Discussion

We have developed a conceptual and methological framework to evaluate the simultaneous contributions of neutrality, forbidden links and sampling effects on the structure of mutualistic networks. We have used this framework to evaluate the influence of relative abundance (neutrality) and spatio–temporal overlap on a pollination network. Although we have not included information on phenotypic trait matching and sampling effects, if available this type of information can be easily incorporated to our conceptual and methodological framework. For example, Stang et al. (2006; 2007; 2009) have derived interaction probabilities based on rules of phenotypic matching between plants and nectar-feeding flower visitors. From such information it would be straightforward to derive a probability matrix to evaluate the relative contribution of phenotypic matching to the structure of the interaction matrix. Similarly, if detection probabilities of particular interactions could be estimated, then a detection probability matrix $\mathbf{E}$ could be incorporated into our framework (our implicit assumption above has been that all interactions have a detection probability of one).

One issue we have not been able to solve is how to incorporate phylogenetic information into our framework. This limitation stems from the difficulty of predicting interaction probabilities based on the independent plant and animal phylogenies, with no reference to the observed interaction matrix. Current methods for the detection of a phylogenetic signal in interaction networks (Ives and Godfray, 2006) use a linear model approach, fitting the phylogenetic variance–covariance matrix to the interaction matrix, and there is currently no way of deriving an expected probability matrix based on the independent phylogenies alone. We hope our efforts can stimulate others to work out a solution to this crucial problem.

Using our conceptual and methodological framework, we have shown that interaction probabilities derived from abundance and temporal overlap predict very closely the aggregate properties of a plant–pollinator network. In contrast, our likelihood analysis shows that information on abundance and spatio–temporal distribution falls short of predicting the detailed network structure, leaving a large amount of variation unexplained. Thus, although information on abundance and spatio–temporal overlap allowed us to construct networks with the same aggregate features of real-world networks, we failed resoundingly when attempting to delve into the details of pairwise species interactions, which is arguably the ecologically and evolutionarily relevant scale of analysis. Taken together, our results suggest that both relative species abundance and complementarity in spatio–temporal distribution contribute substantially to generate observed network patterns, but that this information is by no means sufficient to predict the detailed structure of the interaction network.

Of course, the above results for the Villavicencio network are by no means a general evaluation of the relative contribution of neutrality and forbidden links to the structure of mutualistic networks. Only future studies applying our (or a similar) approach to multiple datasets will allow such general evaluation. Unfortunately, most datasets available to date do not include the sort of detailed information needed for this comparison. Clearly, further progress in the understanding of the determinants of network patterns requires spatio–temporally explicit datasets with detailed natural history information that may allow deriving sensible rules of phenotypic complementarity. We believe this goal will be facilitated if research efforts are focused on a sample of representative study systems with contrasting ecological conditions throughout the world.

Acknowledgments

References

Alarcón, R., N. M. Waser, and J. Ollerton. 2008. Year-to-year variation in the topology of a plant–pollinator interaction network. Oikos **117**:1796–1807.

Almeida-Neto, M., P. R. Guimarães Jr, and T. M. Lewinsohn. 2007. On nestedness analyses: rethinking matrix temperature and anti-nestedness. Oikos **116**:716–722.

Atmar, W. and B. D. Patterson. 1993. The measure of order and disorder in the distribution of species in fragmented habitat. Oecologia **93**:373–382.

Bascompte, J. and P. Jordano. 2007. Plant–animal mutualistic networks: the architecture of biodiversity. Annual Review of Ecology, Evolution and Systematics **38**:567–593.

Bascompte, J., P. Jordano, C. J. Melián, and J. M. Olesen. 2003. The nested assembly of plant-animal mutualistic networks. Proceedings of the National Academy of Sciences USA **100**:9383–9387.

Bascompte, J., P. Jordano, and J. M. Olesen. 2006. Asymmetric coevolutionary networks facilitate biodiversity maintenance. Science **312**:431–433.

Basilio, A. M., D. Medan, J. P. Torretta, and N. J. Bartoloni. 2006. A year-long plant–pollinator network. Austral Ecology **31**:975–983.

Blüthgen, N., J. Fründ, D. P. Vázquez, and F. Menzel. 2008. What do interaction network metrics tell us about specialization and biological traits? Ecology **89**:3387–3399.

Chacoff, N. P., D. P. Vázquez, E. L. Stevani, J. Dorado, and B. Padrón. 2009. The structure of a desert plant–pollinator network. In review .

Dormann, C. F., B. Gruber, and J. Fründ. 2008. The bipartite Package, version 0.5. R Project for Statistical Computing.

Dupont, Y. L., D. M. Hansen, and J. M. Olesen. 2003. Structure of a plant-flower-visitor network in the high-altitude sub-alpine desert of Tenerife, Canary Islands. Ecography **26**:301–310.

Ives, A. R. and H. C. J. Godfray. 2006. Phylogenetic analysis of trophic associations. American Naturalist **168**:E1–E14.

Jordano, P., J. Bascompte, and J. M. Olesen. 2003. Invariant properties in coevolutionary networks of plant–animal interactions. Ecology Letters **6**:69–81.

Morales, J. M. and D. P. Vázquez. 2008. The effect of space in plant-animal mutualistic networks: insights from a simulation study. Oikos **117**:1362–1370.

Olesen, J. M., J. Bascompte, H. Elberling, and P. Jordano. 2008. Temporal dynamics in a pollination network. Ecology **89**:1573–1582.

Ollerton, J., S. D. Johnson, L. Cranmer, and S. Kellie. 2003. The pollination ecology of an assemblage of grassland asclepiads in south africa. Annals of Botany **92**:807–834.

Petanidou, T., A. S. Kallimanis, J. Tzanopoulos, S. P. Sgardelis, and J. D. Pantis. 2008. Long-term observation of a pollination network: fluctuation in species and interactions, relative invariance of network structure and implications for estimates of specialization. Ecology Letters **11**:564–575.

R Development Core Team, 2007. R: A Language and Environment for Statistical Computing. R Foundation for Statistical Computing, Vienna, Austria. URL http://www.R-project.org.

Rezende, E. L., J. E. Lavabre, P. R. Guimarães, P. Jordano, and J. Bascompte. 2007. Non-random coextinctions in phylogenetically structured mutualistic networks. Nature **448**:925–928.

378 Rodríguez-Gironés, M. A. and L. Santamaría. 2006. A new algorithm to calculate the
379   nestedness temperature of presence–absence matrices. Journal of Biogeography
380   **33**:924–935.

381 Roig, F. A. 1972. Bosquejo fisionómico de la vegetación de la provincia de mendoza.
382   Boletín de la Sociedad Argentina de Botánica **13, Suppl.**:49–80.

383 Santamaría, L. and M. A. Rodríguez-Gironés. 2007. Linkage rules for plant–pollinator
384   networks: trait complementarity or exploitation barriers? PLoS Biology **5**:e31.

385 Stang, M., P. G. L. Klinkhamer, and E. van der Meijden. 2006. Size constraints and
386   flower abundance determine the number of interactions in a plant-flower visitor web.
387   Oikos **112**:111–121.

388 Stang, M., P. G. L. Klinkhamer, and E. van der Meijden. 2007. Asymmetric
389   specialization and extinction risk in plant–flower visitor webs: a matter of morphology
390   or abundance? Oecologia **151**:442–453.

391 Stang, M., P. G. L. Klinkhamer, N. M. Waser, I. Stang, and E. van der Meijden. 2009.
392   Size-specific interaction patterns and size matching in a plant-pollinator interaction
393   web. Annals of Botany **103**:000–000.

394 Strauss, S. Y. and R. E. Irwin. 2004. Ecological and evolutionary consequences of
395   multispecies plant-animal interactions. Annual Review of Ecology, Evolution, and
396   Systematics **35**:435–466.

397 Tylianakis, J. M., T. Tscharntke, and O. T. Lewis. 2007. Habitat modification alters the
398   structure of tropical host-parasitoid food webs. Nature **445**:202–205.

399 Vázquez, D. P. and M. A. Aizen. 2003. Null model analyses of specialization in
400   plant-pollinator interactions. Ecology **84**:2493–2501.

401 Vázquez, D. P. and M. A. Aizen. 2004. Asymmetric specialization: a pervasive feature of
402   plant-pollinator interactions. Ecology **85**:1251–1257.

403 Vázquez, D. P., N. Blüthgen, L. Cagnolo, and N. P. Chacoff. 2009. Uniting pattern and
404   process in plant–animal mutualistic networks: a review. Annals of Botany **103**:000–000.

405 Vázquez, D. P., C. J. Melián, N. M. Williams, N. Blüthgen, B. R. Krasnov, and
406   R. Poulin. 2007. Species abundance and asymmetric interaction strength in ecological
407   networks. Oikos **116**:1120–1127.

408 Vázquez, D. P., W. F. Morris, and P. Jordano. 2005. Interaction frequency as a surrogate
409   for the total effect of animal mutualists on plants. Ecology Letters **8**:1088–1094.

Figure legends

Figure 1. Plant–pollinator interaction matrices. (a) Observed plant–pollinator matrix in the Monte desert of Villavicencio Nature Reserve (Mendoza, Argentina). (b) Interaction matrix resulting from one iteration of the randomization algorithm, using the $\overline{\mathbf{NT}}$ probability matrix to assign interactions. In each matrix, rows represent pollinator species, columns represent plant species, and circle diameter of a matrix element y_{ij} is proportional to the square root of the number of interactions between pollinator i and plant j.

Figure 2. Comparison between aggregate network statistics observed in the Villavicencio network and those predicted by the probability matrices. In each panel, the vertical line represents the observed value of an aggregate statistic, the circles represent the value of the statistic expected from each probability matrix, with errorbars indicating 95% confidence intervals. Results are shown for the seven probability matrices resulting from all possible combinations of abundance ($\mathbf{N}$), temporal overlap ($\mathbf{T}$) and spatial overlap ($\mathbf{S}$) and for the null probability matrix with homogeneous interaction probabilities across all pairwise interactions (Null).

Figure 3. Likelihood analysis of pairwise interaction probabilities. Results are shown for three abundance measures (see Methods): (a) density of individuals, (b) density of flowers and (c) density of pollen. Each panel shows the dAIC values corresponding to each of the seven probability matrices resulting from all possible combinations of abundance ($\mathbf{N}$), temporal overlap ($\mathbf{T}$) and spatial overlap ($\mathbf{S}$). The dAIC value for a null probability matrix with homogenous interaction probability across all pairwise interactions (Null) and the observed interaction matrix fitted to itself ($\mathbf{Y}$) are also shown for comparison.

11

(a) Observed matrix

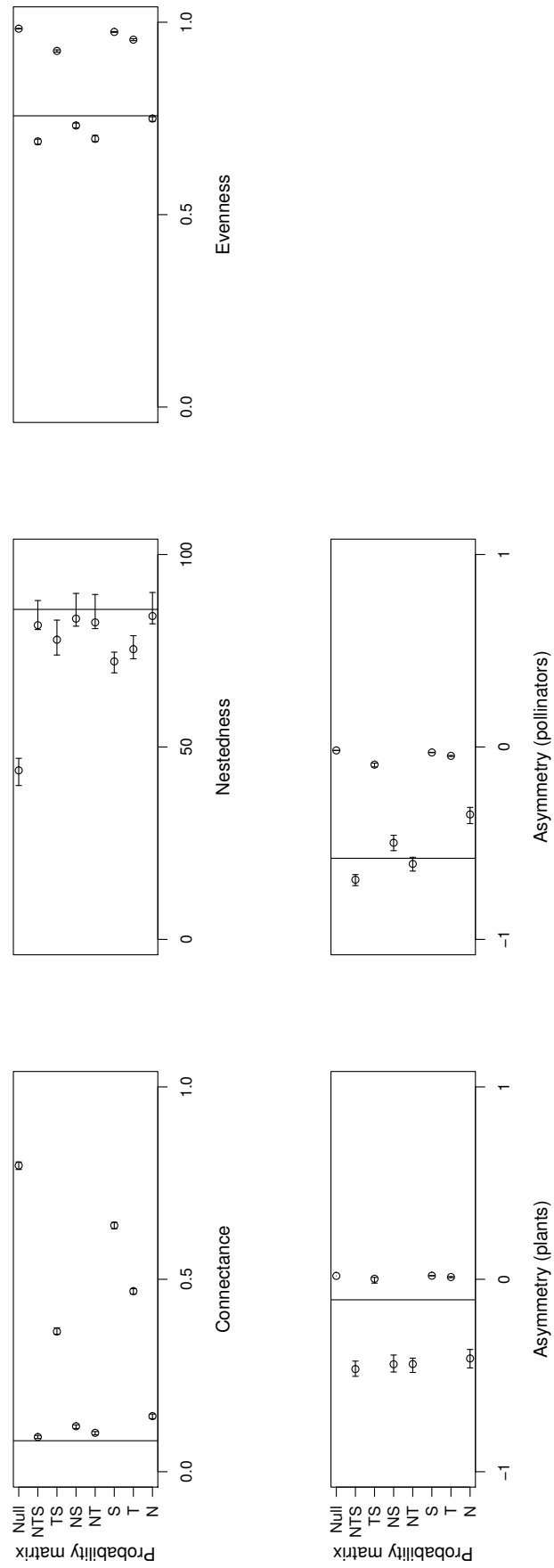(b) Matrix predicted by $\overline{\mathbf{NT}}$
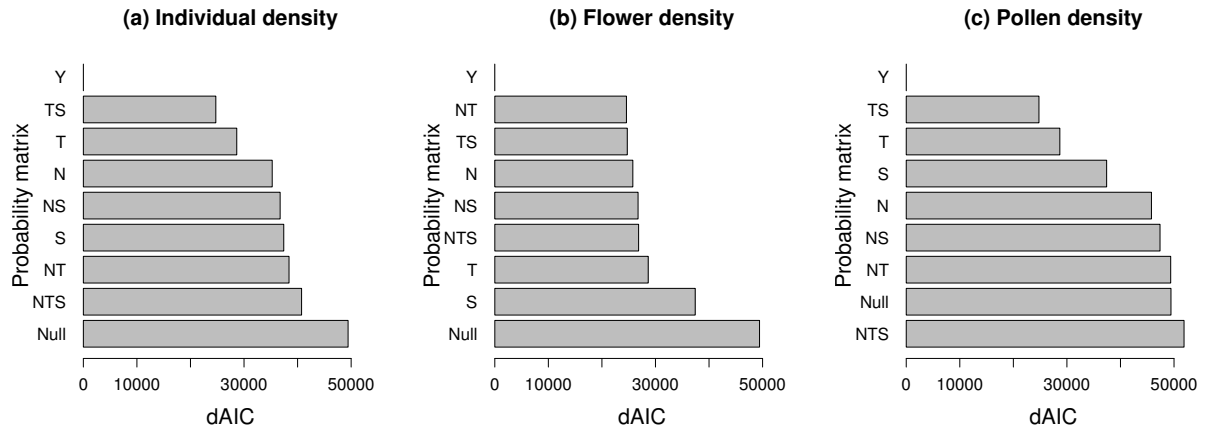
Figure 1:

Figure 2:

Figure 3:

Electronic Appendices

Appendix A. Phylogenetic analyses.

Construction of plant and insect phylogenies. We used the plant phylogenetic database Phylomatic (http://www.phylodiversity.net/phylomatic) to construct the plant phylogeny. Phylomatic is based on the Angiosperm supertree built by Davies et al. (2004), and allows inputting a list of plant species with their family affiliation to obtain a phylogenetic tree. We selected the "conservative seed plant tree" option, which leaves nodes with less of 80% support as soft polytomies. We also chose to estimate pseudo branch lengths, which Phylomatic does by calibration with dates from Wikstrom et al. (2001). The phylogeny returned by Phylomatic (Fig. A1a) was then used to calculate the phylogenetic variance–covariance matrix $\mathbf{U}$ (Cunningham et al., 1998; Garland and Ives, 2000), using the vcv.phylo function in the ape package of R (Paradis et al., 2004).

For the insects, we assembled a family-level phylogeny from the Tree of Life (Maddison and Schulz, 2007). For families with more than two species that could be identified to genus or species, we inserted within-family phylogenies into the family-level phylogeny. Within-family phylogenies were drawn from the Tree of Life and from selected sources: Syrphidae, Ståhls et al. (2003), Mengual et al. (2008); Halictidae, Danforth et al. (2008); Megachilidae, Danforth et al. (2006). As for the plants, this phylogeny (Fig. A1b) was used to calculate the variance–covariance matrix $\mathbf{V}$.

Estimation of phylogenetic signal. We evaluated the strength of the phylogenetic signal of the two phylogenies on the interaction matrices with the methods developed by Ives and Godfray (2006), which use a linear model approach to fit the phylogenetic variance–covariance matrix to the interaction matrix. Ives and Godfray (2006) propose that the matrix of interaction strengths can be described by a linear model, $\mathbf{Y} = b_0 + \epsilon$, where $\mathbf{Y}$ is the interaction matrix in vectorized form (i.e., the result of "stacking" columns into a single column vector), b_0 is the phylogenetically corrected mean of interaction strength, and ϵ is a column vector of the same dimension as $\mathbf{Y}$. Vector ϵ has an associated variance–covariance matrix $E[\epsilon\epsilon'] = \mathbf{W}$, which is a function of the phylogenies of plants and insects. Specifically, $\mathbf{W} = \mathbf{U} \otimes \mathbf{V}$, where $\mathbf{U}$ and $\mathbf{V}$ are the phylogenetic variance–covariance matrices for plants and insects, respectively, and $\otimes$ is the Kronecker product.

The overall strength of the phylogenetic signal can be assessed by comparing the mean squared error (MSE) calculated by fitting the model with the actual data (MSE_d), the MSE derived under the assumption of no phylogenetic covariances (a "star" phylogeny; MSE_star), and the MSE derived assuming maximum phylogenetic signal (i.e., Brownian motion evolution, MSE_b). Lower values of MSE indicate better fit of the specific model to the data (i.e., the model with the lowest MSE leaves the smallest unexplained variance). In addition, the independent signals of the plant and the animal phylogenies, d_p and d_a, can be estimated from b_0 in the linear model. A value of $d = 0$ means no phylogenetic signal, $d = 1$ means maximum phylogenetic signal under the assumption of Brownian motion evolution, and $d > 1$ corresponds to disruptive selection. We used the pblm function in the picante package of R (Kembel et al., 2008) to calculate these measures of phylogenetic signal.

References

Cunningham, C. W., K. E. Omland, and T. H. Oakley. 1998. Reconstructing ancestral character states: a critical reappraisal. Trends in Ecology & Evolution **13**:361–366.

Danforth, B., C. Eardley, L. Packer, K. Walker, A. Pauly, and F. Randrianambinintsoa. 2008. Phylogeny of Halictidae with an emphasis on endemic African Halictinae. Apidologie **39**:86–101.

Danforth, B. N., S. Sipes, J. Fang, and S. G. Brady. 2006. The history of early bee diversification based on five genes plus morphology. Proceedings of the National Academy of Sciences USA **103**:15118–15123.

Davies, T. J., T. G. Barraclough, M. W. Chase, P. S. Soltis, D. E. Soltis, and V. Savolainen. 2004. Darwin's abominable mystery: Insights from a supertree of the angiosperms. Proceedings of the National Academy of Sciences USA **101**:1904–1909.

Garland, T. and A. R. Ives. 2000. Using the past to predict the present: confidence intervals for regression equations in phylogenetic comparative methods. American Naturalist **155**:346–364.

Ives, A. R. and H. C. J. Godfray. 2006. Phylogenetic analysis of trophic associations. American Naturalist **168**:E1–E14.

Kembel, S., D. Ackerly, S. Blomberg, P. Cowan, M. Helmus, and C. Webb, 2008. picante: Tools for integrating phylogenies and ecology. R package version 0.3-0.

Maddison, D. R. and K.-S. Schulz, editors. 2007. The Tree of Life Web Project. Internet address: http://tolweb.org.

Mengual, X., G. Ståhls, and S. Rojo. 2008. First phylogeny of predatory flower flies (Diptera, Syrphidae, Syrphinae) using mitochondrial COI and nuclear 28S rRNA genes: conflict and congruence with the current tribal classification. Cladistics **24**:543–562.

Paradis, E., J. Claude, and K. Strimmer, 2004. APE: analyses of phylogenetics and evolution in R language.

Ståhls, G., H. Hippa, G. Rotheray, J. Muona, and F. Gilbert. 2003. Phylogeny of Syrphidae (Diptera) inferred from combined analysis of molecular and morphological characters. Systematic Entomology **28**:433–450.

Wikstrom, N., V. Savolainen, and M. W. Chase. 2001. Evolution of angiosperms: Calibrating the family tree. Proceedings of the Royal Society B **268**:2211–2220.
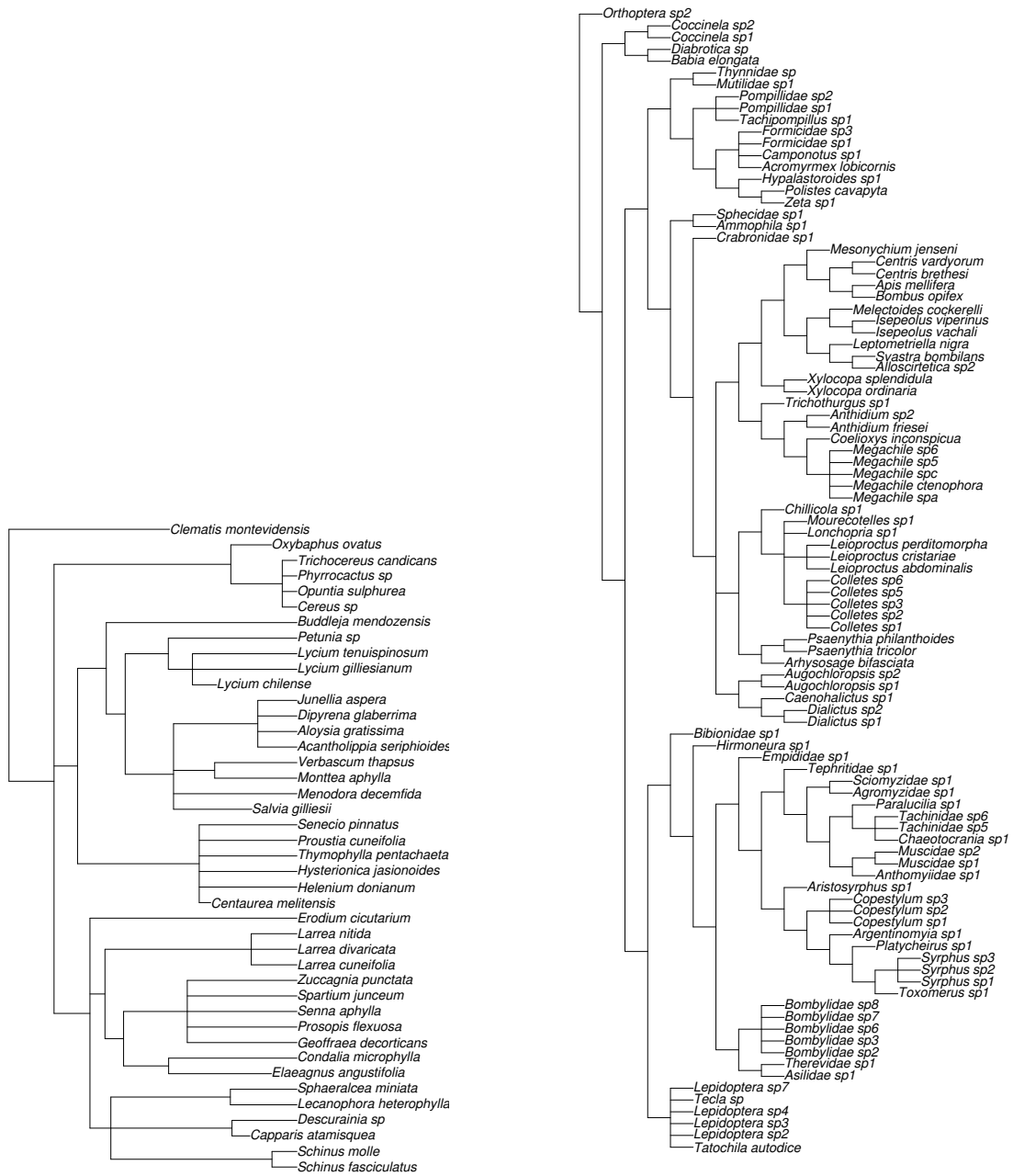
Plant phylogeny

- Clematis montevidensis
- Oxybaphus ovatus
- Trichocereus candicans
- Phyrrocactus sp
- Opuntia sulphurea
- Cereus sp
- Buddleja mendozensis
- Petunia sp
- Lycium tenuispinosum
- Lycium gilliesianum
- Lycium chilense
- Junellia aspera
- Dipyrena glaberrima
- Aloysia gratissima
- Acantholippia seriphioides
- Verbascum thapsus
- Monttea aphylla
- Menodora decemfida
- Salvia gilliesii
- Senecio pinnatus
- Proustia cuneifolia
- Thymophylla pentachaeta
- Hysterionica jasionoides
- Helenium donianum
- Centaurea melitensis
- Erodium cicutarium
- Larrea nitida
- Larrea divaricata
- Larrea cuneifolia
- Zuccagnia punctata
- Spartium junceum
- Senna aphylla
- Prosopis flexuosa
- Geoffraea decorticans
- Condalia microphylla
- Elaeagnus angustifolia
- Sphaeralcea miniata
- Lecanophora heterophylla
- Descurainia sp
- Capparis atamisquea
- Schinus molle
- Schinus fasciculatus

Insect phylogeny

- Orthoptera sp2
- Coccinela sp2
- Coccinela sp1
- Diabrotica sp
- Babia elongata
- Thynnidae sp
- Mutilidae sp1
- Pompillidae sp2
- Pompillidae sp1
- Tachipompillus sp1
- Formicidae sp3
- Formicidae sp1
- Camponotus sp1
- Acromyrmex lobicornis
- Hypalastoroides sp1
- Polistes cavapyta
- Zeta sp1
- Sphecidae sp1
- Ammophila sp1
- Crabronidae sp1
- Mesonychium jenseni
- Centris vardyorum
- Centris brethesi
- Apis mellifera
- Bombus opifex
- Melectoides cockerelli
- Isepeolus viperinus
- Isepeolus vachali
- Leptometriella nigra
- Svastra bombilans
- Alloscirtetica sp2
- Xylocopa splendidula
- Xylocopa ordinaria
- Trichothurgus sp1
- Anthidium sp2
- Anthidium friesei
- Coelioxys inconspicua
- Megachile sp6
- Megachile sp5
- Megachile spc
- Megachile ctenophora
- Megachile spa
- Chillicola sp1
- Mourecotelles sp1
- Lonchopria sp1
- Leioproctus perditomorpha
- Leioproctus cristariae
- Leioproctus abdominalis
- Colletes sp6
- Colletes sp5
- Colletes sp3
- Colletes sp2
- Colletes sp1
- Psaenythia philanthoides
- Psaenythia tricolor
- Arhysosage bifasciata
- Augochloropsis sp2
- Augochloropsis sp1
- Caenohalictus sp1
- Dialictus sp2
- Dialictus sp1
- Bibionidae sp1
- Hirmoneura sp1
- Empididae sp1
- Tephritidae sp1
- Sciomyzidae sp1
- Agromyzidae sp1
- Paralucilia sp1
- Tachinidae sp6
- Tachinidae sp5
- Chaeotocrania sp1
- Muscidae sp2
- Muscidae sp1
- Anthomyiidae sp1
- Aristosyrphus sp1
- Copestylum sp3
- Copestylum sp2
- Copestylum sp1
- Argentinomyia sp1
- Platycheirus sp1
- Syrphus sp3
- Syrphus sp2
- Syrphus sp1
- Toxomerus sp1
- Bombylidae sp8
- Bombylidae sp7
- Bombylidae sp6
- Bombylidae sp3
- Bombylidae sp2
- Therevidae sp1
- Asilidae sp1
- Lepidoptera sp7
- Tecla sp
- Lepidoptera sp4
- Lepidoptera sp3
- Lepidoptera sp2
- Tatochila autodice

(a) Plant phylogeny   (b) Insect phylogeny

Figure A1. Phylogenies of plants and insects included in the plant–pollinator interaction network of Villavicencio Nature Reserve.

Supplement. R functions used for analyses.

Main functions. This supplement contains R functions used for the analyses presented in the main text. Main functions are `plotmat`, which draws plots of the interaction matrices (Fig. 1); `netstats`, which calculates aggregate network statistics (Fig. 2); and `mlik`, which calculates multinomial likelihood and AIC (Fig. 3). Other functions are either called by these main functions to perform operations, or do other related operations.

Function descriptions

`confint` Confidence intervals of a vector or matrix of simulated values. Used by `netstats` to calculate 95% confidence intervals of simulated aggregate network statistics.

`intasymm` Interaction strength asymmetry, calculated following Vázquez et al. (2007).

`intereven` Interaction evenness, calculated following Tylianakis et al. (2007).

`mgen` Matrix generating algorithm used by `netstats` to generate simulated interaction matrices according to a given probability matrix.

`mlik` Calculation of multinomial likelihood and AIC according to a given probability matrix. Usage: `mlik(imatr, m.p, par)`, where `imatr` is the observed interaction matrix, `m.p` is the probability matrix, and `par` is the number of parameters used to calculate AIC.

`netstats` Aggregate network statistics: connectance, nestedness, interaction evenness and mean interaction strength asymmetry for each group in the network. Usage: `netstats(imatr, randomize=TRUE, iter=1000, pmatr=NULL)`, where `imatr` is the observed interaction matrix and `pmatr` is the probability matrix used for generating predicted matrices. The R package `bipartite` (Dormann et al., 2008) is required by `netstats` to calculate nestedness.

`plotmat` Graphic function to plot interaction matrices as in Fig. 1. Usage: `plotmat(imatr, xlabel="PLANTS", ylabel="POLLINATORS", cexmin=0.2, cexmax=2, sortm=TRUE, sqroot=TRUE)`, where `imatr` is the interaction matrix to be plotted, `xlabel` and `ylabel` are the texts for the x and y axes, `cexmin` and `cexmax` are the minimum and maximum sizes of circles representing pairwise interactions, `sortm` indicates whether matrix should be sorted (`sortm=TRUE`) or left in the original order (`sortm=FALSE`), and `sqroot` indicates whether interaction frequencies (matrix cells) are to be plotted in untransformed or square-root transformed.

`quant2bin` Transformation of quantitative matrix into binary. Used by `netstats` to calculate connectance.

`sortmatr` Matrix sorting algorithm used by `plotmat`. The matrix is sorted according to row and column totals, so that nestedness can be visualized.

`sortmatrext` Matrix sorting algorithm used as an alternative to `sortmatr`. Here, the matrix is sorted according to external vectors instead of row and column totals.

References

Dormann, C. F., B. Gruber, and J. Fründ. 2008. Introducing the bipartite package: analysing ecological networks. R News **8/2**:8–11.

Tylianakis, J. M., T. Tscharntke, and O. T. Lewis. 2007. Habitat modification alters the structure of tropical host-parasitoid food webs. Nature **445**:202–205.

Vázquez, D. P., C. J. Melián, N. M. Williams, N. Blüthgen, B. R. Krasnov, and R. Poulin. 2007. Species abundance and asymmetric interaction strength in ecological networks. Oikos **116**:1120–1127.